Colloid Polym Sci 279:1013–1019 (2001)

ORIGINAL CONTRIBUTION

P. E. R. Durigon
D. F. S. Petri
H. Drings
Th. Schimmel
M. Bruns

Characterization and modification of polymer blend films

Received: 11 December 2000
Accepted: 6 April 2001

P. E. R. Durigon · D. F. S. Petri (✉)
Instituto de Química, Universidade
de São Paulo, P.O. Box 26077
05599-970 São Paulo SP, Brazil
e-mail: dfsp@quim.iq.usp.br
Tel.: +55-11-38183831
Fax: +55-11-38155579

H. Drings · Th. Schimmel
Institut für Angewandte Physik
Universität Kalrsruhe (TH)
76133 Karlsruhe, Germany

M. Bruns
Forschungszentrum Karlsruhe GmbH
Institut für Instrumentelle Analytik
P.O. Box 3640, 76021 Karlsruhe, Germany

Abstract Films of immiscible blends of (PS) and poly(methyl methacrylate) (PMMA) were characterized by contact-angle measurements with sessile drop and atomic force microscopy (AFM). These blends showed a linear dependence of the contact angles on the composition, as predicted by Cassie's equation for ideal surfaces. The surface structure investigated by AFM showed low roughness and phase-separation features. The ratio between the drop radius and the roughness amounted to the order of 10^4–10^5. This magnitude seemed to be sufficient to put the PS/PMMA films close to ideality. Upon sulfonation, the wettability and the microscopic surface roughness of the PS/PMMA blends increased. The treatment with sulfuric acid yielded sulfonated PS domains on the surface, causing an increase in the surface wettability. The SO_3^- groups were evidenced by X-ray photoelectron spectroscopy. The sulfonation of the PS/PMMA blends enables the formation of multiphase surfaces with hydrophobic, charged and polar domains.

Key words Contact angle · Polystyrene · Poly(methyl methacrylate) · Atomic force microscopy · X-ray photoelectron spectroscopy

Introduction

Polymeric surfaces have often been modified to gain new chemical groups. These groups, situated at the uppermost layers, should increase the surface energy without changing the bulk properties. The development of strategies for polymer surface modification challenges not only fundamental research but also applied areas. Dry processes, like plasma treatment [1–3], are harmless to the environment; however, it has recently [3] been reported that plasma-treated surfaces suffer degradation and lose their properties upon aging. Wet surface reactions [4–7] cause low material degradation, might be very quick, and the quantity of reactants can be minimized to avoid environmental damage.

In previous work [7] we showed that it is possible to turn hydrophobic polystyrene (PS) surfaces into hydrophilic surfaces by an uncomplicated surface sulfonation reaction. It consists of the coverage of PS films with 96% H_2SO_4 for 30 or 60 s or with 50% H_2SO_4 for 15–60 min. The electrophilic substitution [8] in the aromatic ring yielding SO_3^- groups on the surface promotes the increase in the wettability. X-ray photoelectron spectroscopy (XPS) gave evidence for the presence of sulfur and oxygen on the surface. PS-SO_3^- domains distributed in a PS matrix were observed by fluorescence microscopy after staining with rhodamine. Atomic force microscopy (AFM) showed the PS-SO_3^- domains as clumps about 100 nm high.

In the present work we study the surface characteristics of blend films composed of PS and poly(methyl methacrylate) (PMMA) before and after the sulfonation reaction. PMMA is suitable for this study owing to its physical properties, such as its glass temperature (105 °C), which is close to that of PS, avoiding dewetting phenomena at room temperature. Moreover, PMMA is a glassy polymer as is PS; this is advantageous because the film structures are free from crystallization effects.

The surface structure of such blend films is well reported in the literature [9, 10]. Tanaka et al. [9] showed the dependence of the surface structure on the PS/PMMA film (spin-coated on gold) thickness. In the case of 25-μm-thick films PS migrated to the surface owing to its lower surface energy and well-defined macroscopic phase-separated structure in the bulk. The surface structure of films 100 nm thick showed a dependence on the substrate (gold and silicon wafer) and both PS and PMMA enriched the surface. Ultrathin films (films thinner than twice the radius of gyration, $2R_g$) presented a fine, distinct, phase-separated structure caused by a decrease in the Flory–Huggins parameter and in the degree of chain entanglement. Walheim et al. [10] studied the solvent and substrate effects on the surface structure of PS/PMMA blend films (70–140 nm thick). The degree of solubility and swelling of PS and PMMA in toluene, tetrahydrofuran and methyl ethyl ketone, as well as the solvent evaporation rate, controlled the final surface structure. The substrate surface energy also played an important role. The blend surface structure was governed by the preferential orientation of one phase to the substrate. This system was studied in the present work, but here the dependence of blend composition on the wettability and surface morphology before and after the sulfonation reaction are explored to gain better insight into the reactive process and, thus, into the development of multiphase surfaces.

Experimental

Materials

Sulfuric acid (96 ± 1% H_2SO_4) and analytical grade toluene (Nuclear, São Paulo, Brazil) were used without previous treatment. Silicon wafers were purchased from Crystec (Berlin, Germany). PS ($M_n \sim 200{,}000$ g/mol) was kindly supplied by BASF (Ludwigshafen, Germany). PMMA ($M_n \sim 58{,}000$ g/mol) was synthesized by dispersion polymerization.

Methods

Sample preparation

Pure PS, pure PMMA and the PS/PMMA blends in the compositions of 25, 50 and 75 wt% PS were prepared from solutions in toluene at a concentration of 10 g/l. The polymer films were prepared by spin-coating on Si wafers with a Headway PWM32-PS-R790 spinner (Garland, USA). The wafers, with dimensions of 1.5 cm × 1.5 cm were previously rinsed in a standard manner [7] and dried under a stream of N_2. All coatings were performed with a spinning velocity of 3,000 rpm and a spinning time of 30 s. Half the samples were treated with 96% H_2SO_4 for 60 s, washed with distilled water and dried under N_2.

Ellipsometry

The mean thickness and index of refraction of films were determined at 24 ± 1 °C by means of ellipsometry [11] in a DRE-X02 ellipsometer (Ratzeburg, Germany), equipped with a He–Ne laser (632.8 nm) set at an angle of incidence of 70.0°. The sample characteristics are shown in Table 1. The film thickness values are bigger than $2R_g$, in order to avoid thermal fluctuation effects [12]. The radius of gyration of an unperturbed chain can be calculated by

$$R_g = (Nb^2/6)^{1/2} \quad , \tag{1}$$

where N is the degree of polymerization and b is the average statistical segment length.

The magnitudes of b_{PS} and b_{PMMA} are 0.68 and 0.69 nm, respectively [13], while N_{PS} and N_{PMMA} are 1,920 and 580. By substituting these values in Eq. (1), the values of R_g for PS and PMMA are calculated as 12 and 7 nm, respectively.

Contact-angle measurements

Contact-angle measurements were performed with a homebuilt [14] apparatus equipped with a Casio QV-10 digital camera, which is connected to a computer. Sessile water drops of 4 μl were used for

Table 1 Contact angles values (θ_A, θ_R and $\Delta\theta$) and indices of refraction and thickness determined for polystyrene (*PS*), poly(methyl methacrylate) (*PMMA*) and PS/PMMA blend films before and after the treatment with H_2SO_4

Sample	θ_A(°)	θ_R (°)	$\Delta\theta$ (°)	n (λ = 632.8 nm)	d (nm)
Before treatment with H_2SO_4					
PS	89 ± 1	83 ± 4	5	1.583 ± 0.003	63 ± 2
PMMA	69 ± 3	64 ± 3	5	1.485 ± 0.005	40 ± 1
PS/PMMA (25–75%)	73.5 ± 0.5	70 ± 1	4	1.51 ± 0.07	50 ± 6
PS/PMMA (50–50%)	78.5 ± 0.5	74.5 ± 0.5	4	1.553 ± 0.005	51 ± 1
PS/PMMA (75–25%)	84.5 ± 0.5	81 ± 1	4	1.590 ± 0.004	56 ± 2
After treatment with H_2SO_4					
PS	54 ± 4	34 ± 2	20	1.591 ± 0.005	61 ± 1
PMMA	67 ± 1	65 ± 1	2	1.48 ± 0.01	40 ± 1
PS/PMMA (25–75%)	61 ± 2	59 ± 1	2	1.478 ± 0.006	44.8 ± 0.1
PS/PMMA (50–50%)	60 ± 3	56 ± 3	4	1.55 ± 0.05	48.5 ± 0.5
PS/PMMA (75–25%)	59 ± 1	54 ± 1	5	1.613 ± 0.005	54.9 ± 0.3

the advancing contact angle (θ_A) and then the volume was reduced to 2 μl to measure the receding contact angle (θ_R). At least five samples of the same composition were analyzed at different spots.

Atomic force microscopy

AFM measurements were carried out with an instrument from Park Scientific (Sunnyvale, Calif., USA) equipped with a homebuilt head with a laser deflection detection system in the contact mode in air at room temperature. V-shaped silicon nitride cantilevers with sharpened pyramidal tips and force constants between 0.03 and 0.1 N/m were applied. All AFM images represent unfiltered original data and are displayed in a linear gray scale. At least three samples of the same composition were analyzed at different areas of the surface.

X-ray photoelectron spectroscopy

XPS experiments were performed using an ESCALAB-5 electron spectrometer (VG Scientific, East Grinstead, UK) in an ultrahigh vacuum system with a base pressure of approximately 10^{-10} mbar. The photoelectrons are excited in a sample area of about 50 mm^2 by means of nonmonochromatized Mg Kα radiation at a power of 100 W. The kinetic energies are measured by an 150° hemispherical energy analyzer operating in the constant analyzer energy mode using a pass energy of 20 eV for elemental spectra and a resolution of 1.2 eV for the Au $f^{7/2}$ photopeak. The photoelectron takeoff angle was set to 0° with respect to the sample normal. The binding energy scale was calibrated using a value of 285.0 eV for the contamination C 1*s* photopeak and was controlled by means of the well-known photopeaks of metallic Cu, Ag and Au, respectively.

Results and discussion

PS/PMMA blends

A common method to determine the wettability is the measurement of the contact angle between a solid surface and a sessile drop of a liquid. If the liquid wets the surface, the contact angle will be very small (close to 0°), otherwise the angle will be big (close to 90°). Young's equation was formulated for an ideal (homogeneous, rigid, insoluble and flat) surface in contact with a liquid drop. The equation assumes the equilibrium forces in the system formed by a solid surface a liquid drop and its vapor as follows [14]:

$$\cos\theta_Y = \left(\gamma_{sg} - \gamma_{sl}\right)/\gamma_{lg} \ , \qquad (2)$$

where θ_Y is the Young contact angle, γ_{sg} is the interfacial tension between solid and vapor, γ_{sl} is the interfacial tension between solid and liquid and γ_{lg} is the interfacial tension between the liquid and its vapor.

The difference between θ_A and θ_R is the so-called contact angle hysteresis ($\Delta\theta$). In ideal surfaces $\Delta\theta$ should be zero; however, in real surfaces $\Delta\theta$ is no longer zero and stems from surface roughness or surface heterogeneity. Theoretical works [15–18] show that the rougher the surface, the bigger the hysteresis; θ_A increases and θ_R decreases with increasing roughness. The general assumption [19] is that the surface must be smooth at the 0.1–0.5 μm level. Another general assumption [19] is that the surface must be homogeneous at the 0.1 μm level and above. In a smooth heterogeneous surface, θ_A and θ_R reflect the characteristics of the low-energy phase and of the high-energy phase, respectively. Roughness and heterogeneity lead to a large number of metastable configurations separated by energy barriers. Since the metastable states depend on the height of the energy barriers and the macroscopic vibrational energy of the drop, it is very difficult to distinguish the true minimum of energy from the other metastable states; therefore, the measurement of contact-angle hysteresis can give more information about the surface.

From Young's equation (Eq. 2) one concludes that the wettability depends on the interfacial tension $\gamma_{s/l}$, which is the net result of different interactions between the liquid and the solid surface [20]:

$$\gamma_{sl} = \gamma_s + \gamma_l - 2(\gamma_s^d\gamma_l^d)1/2 - 2(\gamma_s^p\gamma_l^p)1/2 \ . \qquad (3)$$

The two last terms on the right side represent the dispersive forces and the polar components (hydrogen bonding, dipole–dipole and electrostatic interactions), respectively.

The contact-angle measurements obtained for water drops on pure PS and PMMA differed by 20°, as shown in Fig. 1 and Table 1. These values agreed with literature values [21]. Water wetted PMMA better than PS, which can be attributed to the presence of ester groups in the PMMA chains, which are able to build hydrogen bonds with water molecules, lowering the interfacial tension between the solid film and the water drop, γ_{sl}.

Blends composed of PS and PMMA are immiscible over the whole composition range [22]. This is a result of high interfacial tension owing to the absence of favorable interactions between PS and PMMA. The dependence of the advancing and receding contact angles on the blend composition was shown to be a linear one (Fig. 1) and fits Cassie's equation [23], which describes the surface heterogeneity effect on the contact angle. Considering a smooth surface composed of two different

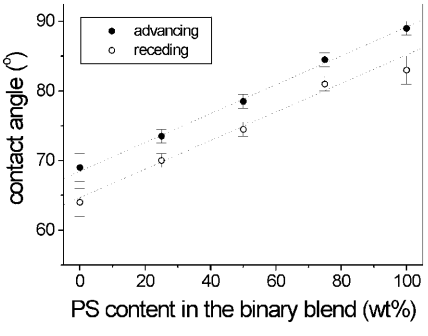

Fig. 1 Contact-angle measurements obtained for water drops on polystyrene (*PS*)/poly(methyl methacrylate) (*PMMA*) blends as a function of the composition

components, Cassie's equilibrium contact angle, θ_C, is a function of the surface composition as follows [20, 23]:

$$\cos\theta_C = Q_{P1}\cos\theta_{P1} + Q_{P2}\cos\theta_{P2} \quad , \tag{4}$$

where Q_{P1} and Q_{P2} are the contents of P1 and P2, respectively, in the surface and θ_{P1} and θ_{P2} are the contact angles for pure P1 and pure P2, respectively. The θ_C (Eq. 4) values cannot be determined exactly because of the metastable states, but they surely lie between the advancing and the receding angles.

AFM images obtained for the PS/PMMA blends showed phase separation over the whole composition range, as shown in Fig. 2. The cross-section analysis (Fig. 2b, d) revealed a topographic structure, where the PMMA phase formed domains about 5–15 nm higher than the region occupied by PS. Tanaka et al. [9] and Walheim et al. [10] observed similar features for the same system under similar conditions. The former proposed that during the spin-coating process residual solvent remains and enables a local surface rearrangement, which is controlled by the substrate/polymer interactions. The latter argued that the formation of the topographic structure during the spin-coating process depends on the relative solubility of the two polymers in the common solvent. One polymer is more quickly depleted of the solvent and freezes earlier than the other. The evaporation of the remaining solvent leads to a further collapse of the better soluble polymer phase. Since toluene swells PS better than PMMA, the PS phase is the collapsed one. Affrossman et al. [24] studied the surface structure of PS/poly(bromostyrene) P(BrS) for a similar preparation (silicon wafer as substrate, toluene as solvent and 4000 rpm as spinning rate). Upon increasing the P(BrS) content in the blend composition, the surface structure changes with formation of islands rich in P(BrS).

The combination of contact-angle and AFM measurements leads to an interesting analysis. From the AFM measurements performed for the PS/PMMA blend films, the microscopic roughness (root-mean-square value) was determined to be 19–30 nm over the whole composition range, for an area of 5 μm × 5 μm. For comparison, bare silicon wafers presented a typical roughness of 0.2 nm. The contact-angle measurements obtained for the PS/PMMA system (Fig. 1) fit well Cassie's model for flat surfaces. The water drop volume of 4 μl yielded on the surface a drop with radius of approximately 1 mm. The ratio between the drop radius and the roughness is of the order of 10^4–10^5. So it seems reasonable to conclude that although the PS/PMMA blend films present a topographic structure, the ratio between the drop radius and the roughness of the order of 10^4–10^5 is still within the limit of Cassie's ideal flat surface. In this way, the PS/PMMA system was shown to have adequate properties to fit the model and the wettability of polymeric blend films obtained from spin-coating predicted by Cassie's equation. Another interesting finding is that there is no dependence of the $\Delta\theta$

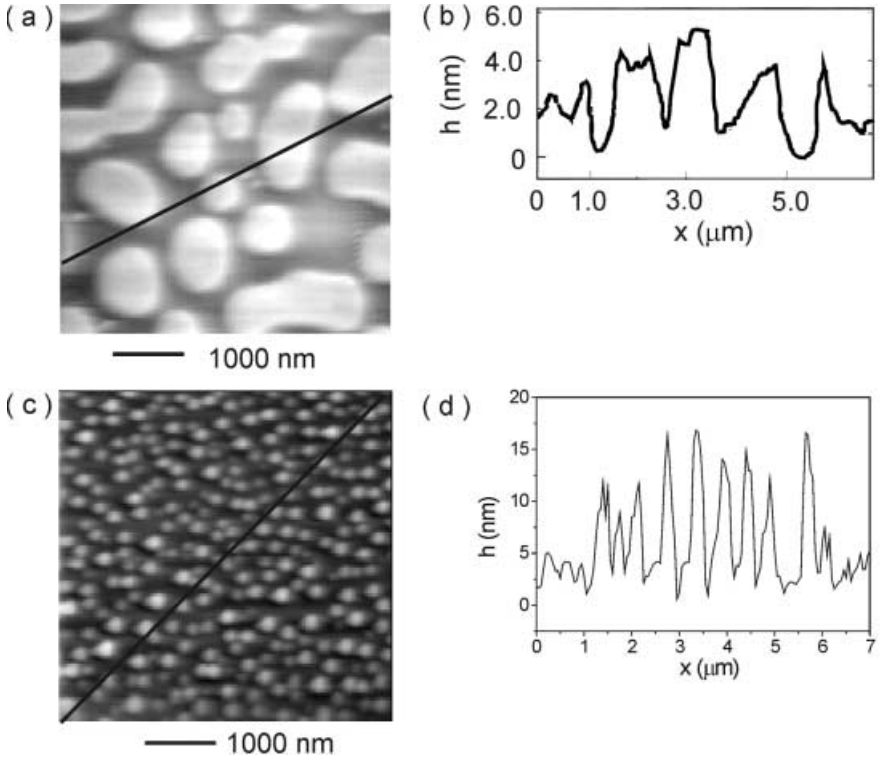

Fig. 2 Atomic force microscopy (*AFM*) images obtained for PS/PMMA with **a** 25% and **b** 75% PS in the composition, with the corresponding cross-section analysis, **b** and **d**

on the surface morphology. Obviously, parameters like solvent polarity, polymer/polymer, polymer/solvent and polymer/substrate interactions have an important role in the surface features and cannot be applied in a general form. Other binary systems will be investigated further.

Modified PS/PMMA blends

After the treatment of pure PMMA with 96% H_2SO_4 there was no considerable change in the advancing and receding contact angles; however, the wettability of the PS/PMMA blends increased significantly, as shown in Fig. 3 and Table 1. Considering the presence of SO_3^- groups on the PS phase owing to the sulfonation in the aromatic ring, the wettability should increase because the charges on the surface increase the polar contribution for the net value of γ_{sl} (Eq. 3). On the other hand, $\Delta\theta$ determined for the PS/PMMA blends before the etching treatment is similar to that obtained after thesurface modification, indicating small changes in themacroscopic roughness; however, the microscopic surface roughness increased to 40–60 nm for an area of 25 μm^2, as determined from AFM images, after the acid reaction. In fact, the sulfonation yielded a ternary blend composed of unreacted PS, unreacted PMMA and sulfonated PS. AFM images for reacted blends with the corresponding cross-section analysis are shown in Fig. 4. By comparing AFM images obtained specially for blends with 75% PS in the composition before and after the sulfonation, Figs. 2c and 4c, respectively, we noticed the presence of additional phase-separation domains dispersed in the PS matrix, which might be attributed to the PS-SO_3^- domains. Such small domains were seldom observed on the surface of PS/PMMA with PS contents less than 50%. The cross-section analysis showed that the additional domains were, on average, smaller (in diameter) and lower than the PMMA domains. This feature is better depicted in Fig. 5. For comparison, the image of pure sulfonated PS is presented in Fig. 6. Even the pure PS surface does not suffer a complete sulfonation of the PS surface. The result is a random phase separation of PS and PS-SO_3^-, as already described in our previous work [7].

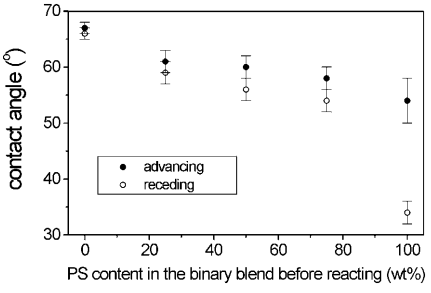

Fig. 3 Contact-angle measurements obtained for water drops on sulfonated PS/PMMA blends as a function of the composition

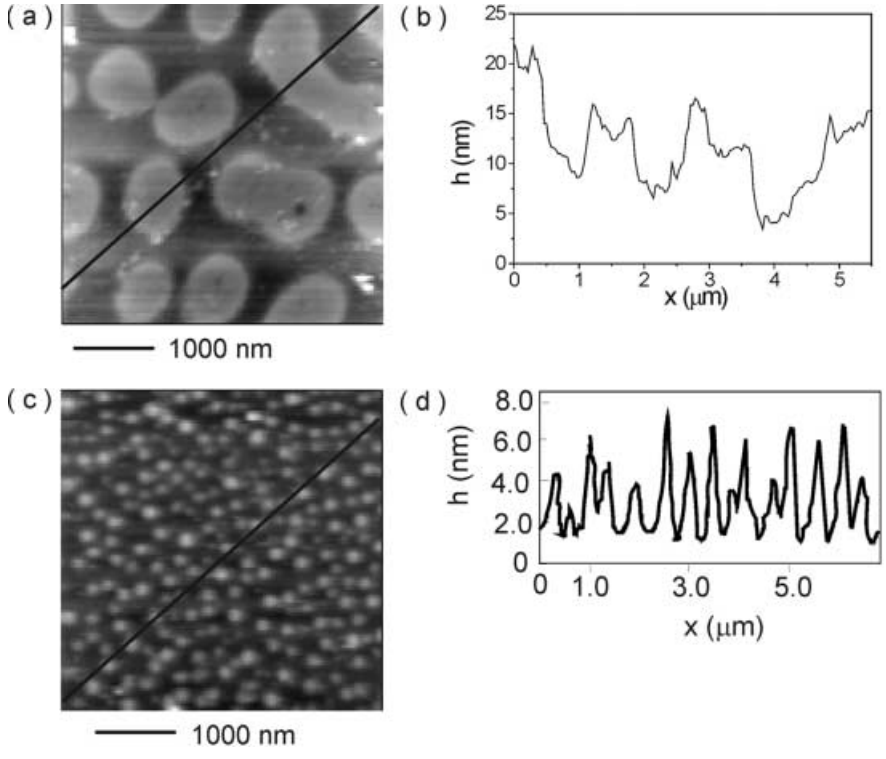

Fig. 4 AFM images obtained for the sulfonated PS/PMMA with **a** 25% and **c** 75% PS in the composition, with the corresponding cross-section analysis, **b** and **d**

The presence of sulfur on the surface of sulfonated pure PS and of blends with 75% PS in the composition was proved by XPS measurements, as shown in Fig. 7a and b, respectively. The photopeaks at 169.8 eV corresponded to the spin orbital S $2p^{1/2}$. The signal intensity obtained for the sulfonated pure PS is higher than that for the blend, indicating that just a small portion of the PS phase reacts. This result corroborates with the low islands observed in Figs. 4c and 5. Moreover, the high PMMA domains might hinder sterically the reaction. Consequently, the sulfur photopeak intensity observed for the blends was too low to enable a quantitative analysis. For blends with PS contents lower than 50% the sulfonation effect was too low to be detected by either AFM or XPS analysis.

The indices of refraction and thickness values determined for the PS/PMMA blends after the H_2SO_4 etching are slightly different from those obtained for the samples before the treatment. These small changes are probably due to the increase in roughness.

Conclusions

The binary polymer blends composed of PS and PMMA presented smooth surfaces and a linear dependence of advancing and receding angles on the composition, fitting Cassie's equation, while no dependence of the contact-angle hysteresis on the surface topography was observed. The sulfonation of the PS/PMMA binary blends yielded ternary blends composed of PMMA, PS and PS-SO_3^-. A significant increase in wettability could be observed for blends with 50% PS or more, owing to the presence of the SO_3^- groups on

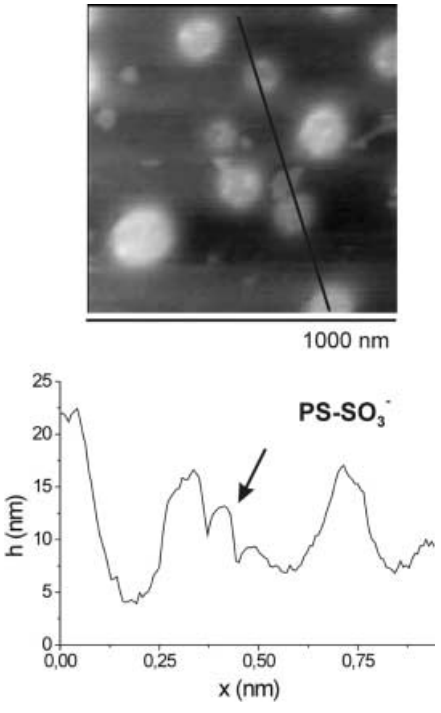

Fig. 5 Zoom AFM image for the sulfonated PS/PMMA with 75% PS in the composition, with the corresponding cross-section analysis

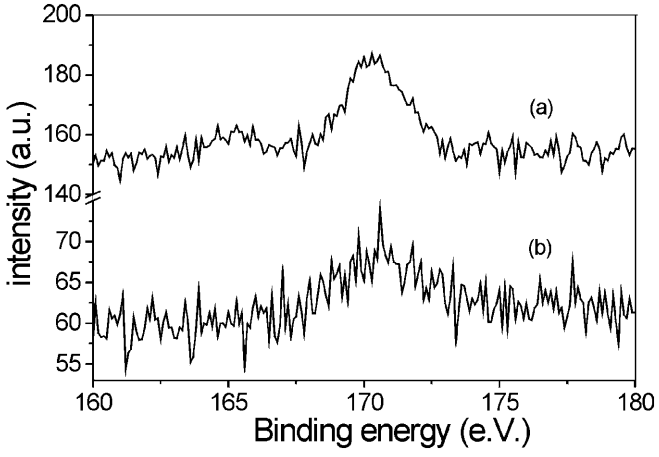

Fig. 7 X-ray photoelectron spectroscopy measurement of S 2*p* obtained for the surface of **a** sulfonated pure PS and **b** of sulfonated blends with 75% PS in the composition

Fig. 6 AFM images obtained for the sulfonated PS, with the corresponding cross-section analysis

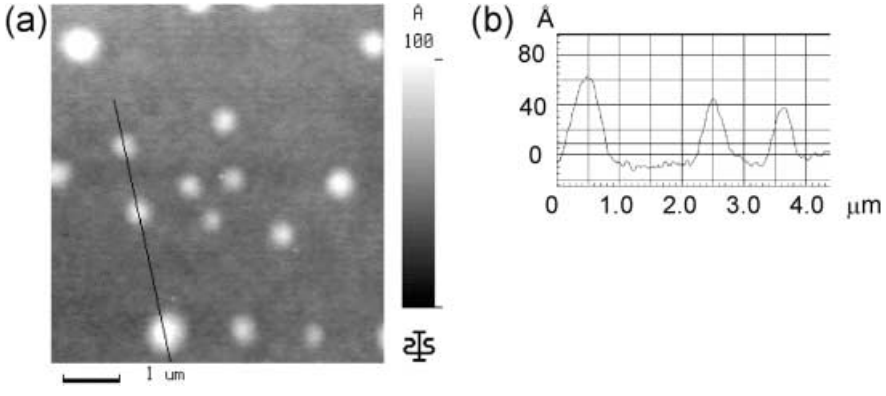

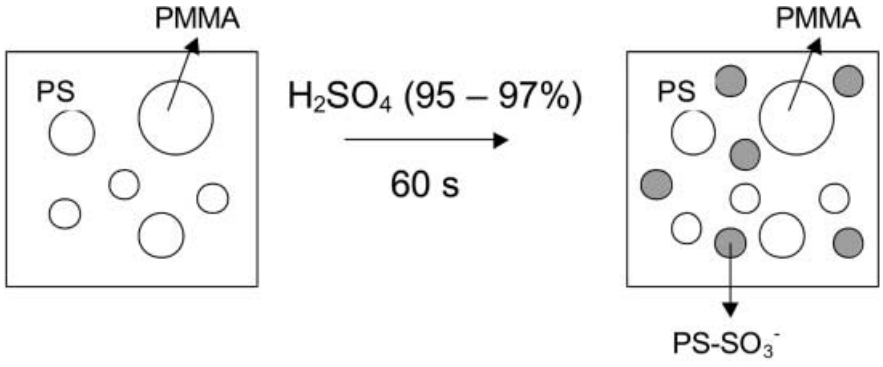

Fig. 8 Schematic representation of the creation of PS/PMMA PS-SO_3^- by means of the sulfonation reaction

the surface. These ternary blends are interesting systems because their surfaces can be easily tailored by the composition variation and the selective reaction of PS with sulfuric acid. The surface schematic representation (Fig. 8) before and after the sulfonation reaction depicted the creation of a surface with hydrophobic sites (unreacted PS), domains with marginal polarity (PMMA) and charged domains. The surface character can be easily controlled by the blend composition. If charges are desired, the PS content should be high, since only PS is transformed in PS-SO_3^-. The application of such surfaces as substrates might be especially interesting for selective adsorption process, involving charged adsorbates, like proteins and polyelectrolytes.

Acknowledgements P.E.R.D and D.F.S.P. acknowledge FAPESP and CNPq for financial support.

References

1. Idage SB, Badrinarayanan S (1998) Langmuir 14:2780
2. Keller D, Schröder K, Husen B, Ohl A (1997) Polym Prepr Am Chem Soc Div Polym Chem 38:1043
3. Dupont-Gillain CC, Adriaensen Y, Derclaye S, Rouxhet PG (2000) Langmuir 16:8194
4. Rao BS, Puschett JB, Matyjaszewski K (1991) J Appl Polym Sci 43:925
5. Feng Y, Karim A, Weiss RA, Douglas JF, Han CC (1998) Macromolecules 31:484
6. Gibson HW, Bailey FC (1980) Macromolecules 13:34
7. Siqueira-Petri DF, Wenz G, Schunk P, Schimmel T, Bruns M, Dichtl M (1999) Colloid Polym Sci 277:673
8. March J (1992) Advanced organic chemistry: reactions, mechanisms and structures. Wiley, New York, p 528
9. Tanaka K, Takahara A, Kajiyama T (1996) Macromolecules 29:3232
10. Walheim S, Böltau M, Mlynek J, Krausch G, Steiner U (1997) Macromolecules 30:4995
11. Azzam RMA, Bashara NM (1987) Ellipsometry and polarized light. North Holland, Amsterdam
12. Tanaka K, Yoon JS, Takahata A, Kajiyama T (1995) Macromolecules 28:934
13. Ballard DGH, Wignall GD, Schelten J (1973) Eur Polym J 9:965
14. Adamson A (1982) Physical chemistry of surfaces. Wiley, New York
15. Wolansky G, Marmur A (1998) Langmuir 14:5292
16. Marmur A (1998) Colloids Surf A 136:209
17. Marmur A (1994) J Colloid Interface Sci 168:40
18. Morra M, Occhiello E, Garbassi F (1989) Langmuir 5:872
19. Andrade JD (1985) Surface and interfacial aspects of biomedical polymers, vol 1. Plenum, New York, pp 139–185
20. Garbassi F, Morra M, Occhiello E (1992) Polymer surfaces: from physics to technology. Wiley, New York
21. Chaudhury MK (1996) Mater Sci Eng Rev 16:97
22. Kozlowski M, Skowronski T (1984) In: Kryszewski A, Galeski A, Martuscelli E (eds) Polymer blends: processing, morphology and properties, vol 2. Plenum, New York, p 101–109
23. Cassie ABD (1948) Discuss Faraday Soc 3:11
24. Affrossman S, Henn G, O'Neil SA, Pethrick RA, Stamm M (1996) Macromolecules 29:5010